

Gravity waves in the troposphere and stratosphere during the MaCWAVE/MIDAS summer rocket program

A. Schöch¹, G. Baumgarten¹, D. C. Fritts², P. Hoffmann¹, A. Serafimovich¹, L. Wang², P. Dalin³, A. Müllemann¹, F. J. Schmidlin⁴

Combining data taken during the MaCWAVE summer rocket campaign at the Andøya Rocket Range (69.3° N, 16.0° E) with a lidar, radiosondes, falling spheres, and VHF radars at Andøya and at the Esrange, the gravity wave content of the troposphere and stratosphere during the campaign nights was analyzed. The lidar yielded vertical wavelengths and periods of gravity waves in the stratosphere. A hodograph analysis was performed for the radiosonde and falling sphere data to estimate propagation directions of the gravity waves. The wave content in the troposphere was inferred by applying wavelet and cross-spectral methods to the radar data. We found propagation conditions and spectra of the waves to vary with height following the change in the background wind. The waves were excited both at the ground and in the tropopause/lower stratosphere region. The dominant waves had observed periods of ~ 2 to 12 hours and vertical wavelengths from a few to some 10's of kilometer.

1. Introduction

Without the gravity wave dissipation in the mesopause region the polar mesopause temperature in summer of ~ 130 K would be ~ 90 K warmer [e.g. Garcia and Solomon, 1985]. The momentum deposition by gravity waves accounts for the residual circulation from the summer to the winter pole by introducing an ageostrophic flow. The residual circulation induces adiabatic cooling of ~ 50 K d^{-1} by a mean vertical upwelling of ~ 5 $cm\ s^{-1}$ [e.g. Fritts and Luo, 1995] and the resulting thermal structure approaches an adiabatic temperature gradient in the upper mesosphere.

In July 2002 a comprehensive study of gravity waves and turbulence was conducted at the Andøya Rocket Range (ARR) in Northern Norway (69.3° N, 16.0° E). The international MaCWAVE/MIDAS campaign (for a detailed description of the campaign see Goldberg *et al.* [2003]) involved launches of sounding rockets, meteorological rockets (falling spheres), and balloons together with the ground based VHF and MF radars as well as the Rayleigh and sodium resonance lidars at the ALOMAR research facility and the Esrange MST radar in Kiruna.

While many aspects of gravity waves have been studied in great depth already [e.g. Fritts and Alexander, 2003], the

MaCWAVE/MIDAS campaign provided a unique opportunity to investigate gravity waves over the entire height range from the ground up to 110 km. By fortune, the campaign took place in a year of extraordinary background conditions in the mesopause region (see Goldberg *et al.* [2004] and Becker *et al.* [2004], this issue) which were accompanied by strong turbulence below the mesopause; in fact turbulence in the mesosphere was seen for the first time below 80 km [Rapp *et al.*, 2004, this issue]. Furthermore remarkably large temperature gradients were observed above the mesopause [Fritts *et al.*, 2004, this issue].

This analysis focuses on the observation of gravity wave excitation and propagation in the troposphere and stratosphere and investigates whether the observed exceptional mesopause conditions are accompanied by an exceptionally high local gravity wave activity in the lower parts of the atmosphere.

We continue with a short description of the different instruments, the available data and the data processing methods. The results from the different instruments and the additional information that can be gained by combining these data sets are described in section 3. Finally, conclusions from this joint study of gravity waves in the troposphere and stratosphere are presented in section 4.

2. Instruments and Data Analysis Techniques

The ALOMAR RMR lidar is situated 1.5 km south of the ARR. It uses two 1.8 m diameter tiltable telescopes and Nd:YAG lasers to measure relative density profiles and aerosol properties in the stratosphere and mesosphere during day and night [von Zahn *et al.*, 2000]. Temperature profiles are derived from the density profiles measured with the 532 nm channel between 25 km and 50 km assuming hydrostatic equilibrium. The RMR lidar provided continuous data coverage during both salvos of the rocket campaign. The lidar also operated for extended times before and after the salvos enabling us to compare the salvo nights to the rest of the summer.

The RMR lidar data was averaged over one hour intervals. The necessary filters to achieve the needed daylight capability of the lidar reduce the signal strength and restrict the usable height range. A 1.5 km filter was applied to the derived temperature profiles to reduce uncertainties. The wave components T' were determined by subtracting the nightly mean profile \bar{T} from the single temperature profiles ($T' = T - \bar{T}$). This gives an effective bandwidth of 1 – 14 hours in time and 1.5 km – 25 km in vertical wavelength where the upper limits are given by the length and the altitude range of the data set. The temporal development of the wave structure for the second salvo is shown in Fig. 1. A Fourier transform has been applied to yield spectra of vertical wavelengths and observed periods.

Balloons were launched by a NASA team from the town of Andenes, about 4 km northeast of the ARR, roughly every two hours with six launches during salvo 1 between

¹Leibniz-Institute of Atmospheric Physics, Kühlungsborn, Germany

²Colorado Research Associates, a division of Northwest Research Associates, Boulder, CO, USA

³Swedish Institute of Space Physics, Kiruna, Sweden

⁴NASA/Wallops Flight Facility, Wallops Is., VA, USA

15:44 UT, July 1, and 02:13 UT, July 2, and another six launches during salvo 2 between 17:50 UT, July 4, and 04:12 UT, July 5. Most balloons reached an altitude of more than 35 km. Winds were weak during both salvos so the balloons did not drift very far from the launch site. The falling sphere technique was used to measure temperatures between 36 km and 85 km and winds between 36 km and 80 km [Schmidlin, 1991; Müllemann, 2004]. The launch schedule is described in detail by Goldberg *et al.* [2003]. For this work, wind and temperature profiles from the falling spheres were used to cover the altitude range from 36 km to the stratopause.

A directionality analysis was performed on the radiosonde and falling sphere profiles following closely Allen and Vincent [1995] and Vincent *et al.* [1997]. For each individual sounding, an upper stratospheric segment (36 km–50 km) was defined for gravity wave analysis of the rocket data, while lower stratospheric (15 km–25 km) and tropospheric (2 km–8 km) segments were defined for the balloon profiles. The segments were chosen to exclude the stratopause and tropopause regions to achieve approximately constant Brunt-Väisälä frequencies in each segment to facilitate the interpretation of the results [Allen and Vincent, 1995].

For the balloon soundings, the mean profiles of the zonal and meridional winds and temperature ($\bar{u}, \bar{v}, \bar{T}$) were estimated using second-order polynomial fits within the given altitude ranges. For the rocket data, we calculated the arithmetic averages of the soundings for the particular salvo which were then smoothed by a 7 km low-pass filter to obtain ($\bar{u}, \bar{v}, \bar{T}$). This procedure both smoothed over high-wavenumber noise due to frequent sampling by the balloon payload at lower altitudes and preserved gravity wave variance at periods longer than the duration of the salvo.

Again, the gravity wave perturbations (u', v', T') were assumed to be the differences between the original sounding profiles and the mean profiles (e.g. $u' = u - \bar{u}$). The perturbation profiles were filtered by a 2 km, and a 1 km low-pass filter, respectively, before they were subjected to the directionality analysis. This eliminated contributions to the propagation directions from very short scale perturbations and statistical noise.

For each altitude segment, the averaged gravity wave kinetic energy density K_e was approximated neglecting the vertical velocity contribution by $K_e = \frac{1}{2}(u'^2 + v'^2)$.

The horizontal wave propagation direction (i.e. its phase velocity) can be determined objectively with the Stokes-parameter technique for gravity waves [Vincent and Fritts, 1987]. It determines the horizontal propagation direction from the wind perturbations u' and v' . The remaining ambiguity of 180° is resolved by including the temperature perturbations T' in the analysis. The filtering described above was designed to ensure that the directionality analysis was weighted towards those motions at the largest vertical scales contributing most to the gravity wave kinetic energy.

Additionally, VHF radar wind measurements from two sites west and east of the Scandinavian mountain ridge were used to investigate the gravity wave content in the troposphere and lower stratosphere. The ALOMAR VHF radar (ALWIN, Latteck *et al.* [1999]) and the Esrange MST radar (ESRAD, Chilson *et al.* [1999]) in Kiruna (67.9° N, 21.1° E) are separated by about 250 km, but are otherwise similar in their antenna configurations, frequencies, resolution (300 m and 2 min in height and time, respectively), altitude coverage (2 km–13 km), and measurement mode. Wind measurements are carried out in the Spaced Antenna mode using the Full Correlation Analysis method. Tropospheric and lower stratospheric wind data are available from the ALWIN radar for the whole of July 2002. ESRAD data are available from 3 July, 2002, 07:00 UT onward.

The radar data were averaged for 30 min intervals to reduce noise and account for data gaps caused by switching

between measurements in the troposphere and mesosphere. Analyses were applied to estimate the zonal and meridional wind components from both radar sites. Wavelet transforms were used to determine the scales of the primary waves. As above, a band-pass filter was employed to exclude waves outside the 2–15 hr period and 2–4.5 km vertical wavelength bands. The rotary spectrum technique was used to determine the vertical propagation directions. Finally, a complex cross-spectral analysis of the zonal wind perturbations at both sites was performed to evaluate those gravity waves observed jointly on both sides of the Scandinavian mountain ridge.

3. Results

Comparing the two salvo nights to the other measurements of the RMR lidar during summer 2002, the local wave activity in the stratosphere was below average during salvo 1 and considerably above average during salvo 2; therefore we concentrate our analysis on the latter. In the upper mesosphere large fluctuations, strong turbulence and large gradients were observed during both salvos [Rapp *et al.*, 2004; Fritts *et al.*, 2004, (this issue)].

The temperature perturbations measured with the RMR lidar during salvo 2 (July 4/5) are shown in Fig. 1 and are dominated by a gravity wave with an observed period of ~ 12 hr, a vertical wavelength of ~ 28 km, and an inferred vertical phase speed of -0.7 ms^{-1} . This wave is present over the entire altitude range as indicated by the spectral analysis shown in Fig. 2 (upper panel). Below 33 km and near 50 km, other waves with observed periods between 2 hr and 8 hr are present as well. The suppression of waves with periods smaller than 4 hr between 33 km and 45 km may be connected to a change in wind direction from 200° below 20 km to 80° above 30 km as indicated by the balloon data (Fig. 2 in the article by Goldberg *et al.* [2004], this issue) changing the filtering for the ascending waves. The lower panel of Fig. 2 shows the mean vertical wavelengths spectrum for salvo 2. The nearly continuous shape of the spectrum suggests a superposition of many waves with a wide range of vertical wavelengths. In the wavelength band 1.5 km–4 km, the observed mean spectrum follows the expected k^{-3} dependence [e.g. Fritts and Alexander, 2003].

The horizontal propagation directions for gravity waves derived from the balloon and falling sphere profiles are shown in Fig. 3. In the troposphere and lower stratosphere gravity wave propagation is nearly isotropic. This may be related to the relatively weak winds in the region (zonal winds are generally less than 10 ms^{-1} except directly at the tropopause where a jet developed during the night of salvo 2) and the proximity to the gravity wave source levels and is consistent with previous studies at high latitudes [e.g. Wang, 2003]. The kinetic energy density K_e increases with altitude, agreeing with theoretical expectations. In the upper stratosphere, waves generally propagate eastward during both salvos. The isotropic gravity wave distribution at lower levels combined with westward wind speeds of -13 ms^{-1} to -25 ms^{-1} (see Fig. 2 of Goldberg *et al.* [2004]) in the stratosphere, suggest that ascending westward propagating gravity waves have been filtered out by the background winds due to the critical level effect [Fritts and Alexander, 2003]. This change in the observed propagation directions occurs around the same altitude where we detected a change in the gravity wave spectrum (Fig. 2).

The radar detected wave patterns in both zonal and meridional wind components with maximum amplitudes

around 2 ms^{-1} during salvo 1 and up to 6 ms^{-1} during salvo 2 in agreement with the larger wave activity in the stratosphere during salvo 2 observed with the RMR lidar. Fig. 4 (left panel) displays the time-series of observed periods at a height of 8.1 km calculated using a wavelet transform. It shows waves with observed periods of ~ 5 hr to ~ 11 hr appearing in the evening of July 4, and extending until July 7. The cross-spectral analysis performed on the radar data from the two sites (Fig. 4, right panel) indicates that the spectrum was similar above Kiruna and the coherence greatest for waves with observed periods of ~ 6 hr and ~ 11 hr. From the observed phase differences, the estimated horizontal wavelength was ~ 400 km and ~ 600 km with propagation directions of $\sim 58^\circ$ and $\sim 74^\circ$ towards NE and ENE, respectively. At Andenes, we infer from the rotary spectra averaged over the height range 2 km–4.5 km (not shown here) that the 5 hr wave had a vertical wavelength of ~ 2.7 km and propagated downward while the 11 hr wave had a vertical wavelength of ~ 3.2 km and propagated upward.

Combining this with the upward propagation of the 11 hr wave in the stratosphere observed with the RMR lidar, we conclude that the excitation level for the short-periodic waves must have been in the tropopause or lower stratosphere region while the longer-period wave was excited in the troposphere or orographically. A very detailed and complex analysis of the radiosonde data might reveal the excitation altitude more precisely but is beyond the scope of this work. Comparing RMR lidar and radiosonde or falling sphere data shows that the latter are very sensitive for waves with small scales while the RMR lidar (due to the necessary integration time) only shows waves at larger scales.

4. Conclusions

During the two salvo nights, data from a lidar, balloons, falling spheres and radars have been combined to analyze gravity waves in the troposphere and stratosphere. Both radar and lidar data showed gravity waves with observed periods of 2–12 hours and vertical wavelengths from a few to 10's of kilometer, with the larger scales having larger amplitudes. While the wave propagation directions were rather isotropic in the troposphere and lower stratosphere, there was a dominant eastward propagation direction in the upper stratosphere. These changing propagation directions are consistent with the change in the background wind with altitude. From the radar and lidar data we conclude that the wave source for short-periodic waves must have been in the tropopause or lower stratosphere region while waves with longer periods were excited in the troposphere or at the ground. A cross-spectral analysis for the two radar sites showed strongly correlated waves above Andenes and Kiruna with observed periods of ~ 6 hr and ~ 11 hr.

The combination of radiosonde, falling spheres and continuously operating radar and lidar instruments allows a comprehensive study of gravity wave excitation and propagation in the troposphere and stratosphere. Only the joint use of these instruments reveals the excitation height and mechanism for gravity waves propagating through the troposphere and middle atmosphere. Using the results from this case study, we will now analyze other measurements available from the ALOMAR instruments to find out whether the summer 2002 was special primarily as a result of hemispheric coupling [Becker et al., 2004] or also in the gravity wave activity in the lower atmosphere.

Acknowledgments. We would like to thank the staff at the Andoya Rocket Range, at ALOMAR, and the NASA Wallops

Flight Facility team for providing excellent support. This work was supported by the EU commission through the ALOMAR ARI program. Support for D. C. Fritts and L. Wang was provided by NASA under contracts NAG5-01075 and NAS5-02036.

References

- Allen, S. J., and R. A. Vincent, Gravity wave activity in the lower atmosphere: Seasonal and latitudinal variations, *J. Geophys. Res.*, *100*(D1), 1327–1350, 1995.
- Becker, E., A. Müllemann, F.-J. Lübken, H. Körnich, P. Hoffmann, and M. Rapp, Modulation of the general circulation of the MLT by high Rossby-wave activity in austral winter 2002, *Geophys. Res. Lett.*, 2004.
- Chilson, P., S. Kirkwood, and A. Nilsson, The Esrange MST radar: A brief introduction and procedure for range validation using balloons, *Radio Sci.*, *34*, 427–436, 1999.
- Fritts, D. C., and M. J. Alexander, Gravity wave dynamics and effects in the middle atmosphere, *Rev. Geophys.*, *41*(1), 3/1–64, 2003.
- Fritts, D. C., and Z. Luo, Dynamical and radiative forcing of the summer mesopause circulation and thermal structure – 1. Mean solstice conditions, *J. Geophys. Res.*, *100*(D2), 3119–3128, 1995.
- Fritts, D. C., B. P. Williams, C.-Y. She, J. D. Vance, M. Rapp, F.-J. Lübken, A. Müllemann, and R. A. Goldberg, Observations of extreme temperature and wind gradients near the summer mesopause over Andøya, Norway, *Geophys. Res. Lett.*, submitted, 2004.
- Garcia, R. R., and S. Solomon, The effect of breaking gravity waves on the dynamics and chemical composition of the mesosphere and lower thermosphere, *J. Geophys. Res.*, *90*, 3850–3868, 1985.
- Goldberg, R. A., et al., The MacWAVE program to study gravity wave forcing of the polar mesosphere during summer and winter, in *Proceedings 16th ESA Symposium on European Rocket and Balloon Programmes and Related Research*, vol. ESA SP-530, edited by B. Warmbein, pp. 345–350, 2003.
- Goldberg, R. A., et al., The MacWAVE/MIDAS rocket and ground-based measurements of polar summer dynamics: Overview and mean state structure, *Geophys. Res. Lett.*, submitted, 2004.
- Latteck, R., W. Singer, and H. Bardey, The ALWIN MST radar - Technical design and performances, in *Proceedings 14th ESA Symposium on European Rocket and Balloon Programmes and Related Research*, vol. ESA SP-437, edited by B. Kaldeich-Schürmann, pp. 179–184, Potsdam, Germany, 1999.
- Müllemann, A., Temperature, Winde und Turbulenz in der polaren Sommermesosphäre, Ph.D. thesis, Universität Rostock, Rostock, Germany, 2004.
- Rapp, M., B. Strelnikov, A. Müllemann, F.-J. Lübken, and D. C. Fritts, Turbulence measurements and implications for gravity wave dissipation during the MacWAVE/MIDAS rocket program, *Geophys. Res. Lett.*, 2004.
- Schmidlin, F. J., The inflatable sphere: A technique for the accurate measurement of middle atmosphere temperatures, *J. Geophys. Res.*, *96*(D12), 22,673–22,682, 1991.
- Vincent, R. A., and D. C. Fritts, A climatology of gravity wave motions in the mesopause region at Adelaide, Australia, *J. Atmos. Sci.*, *44*, 748–760, 1987.
- Vincent, R. A., S. J. Allen, and S. D. Eckermann, Gravity-wave parameters in the lower stratosphere, in *Gravity wave processes: Their parameterization in global climate models*, edited by K. Hamilton, pp. 7–25, Springer-Verlag, 1997.
- Wang, L., Gravity wave analysis of four years of high vertical resolution U.S. radiosonde data, Ph.D. thesis, Stony Brook University, Stony Brook, NY, USA, 2003.
- von Zahn, U., G. von Cossart, J. Fiedler, K. H. Fricke, G. Nelke, G. Baumgarten, D. Rees, A. Hauchecorne, and K. Adolfsen, The ALOMAR Rayleigh/Mie/Raman-lidar: objectives, configuration, and performance, *Ann. Geophys.*, *18*, 815–833, 2000.

A. Schöch, Leibniz-Institute of Atmospheric Physics, Schloßstraße 6, D-18225 Kühlungsborn, Germany. (schoech@iap-kborn.de)

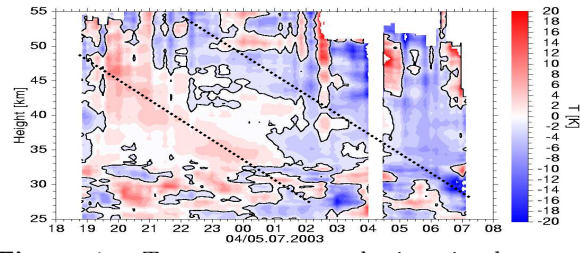


Figure 1. Temperature perturbations in the stratosphere during salvo 2 from RMR lidar data (gap around 4 am caused by drifting clouds). Dominating wave phases are marked with dotted lines.

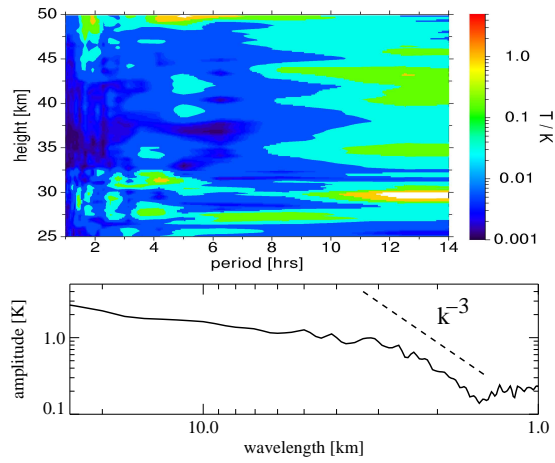


Figure 2. Upper panel: Spectra of observed wave periods for salvo 2 from RMR lidar data in Fig. 1. Lower panel: Mean vertical wavelength spectrum for salvo 2 from RMR lidar data. A theoretically expected k^{-3} dependence (dashed line) is found in the wavelength band 1.5–4 km (see text for details).

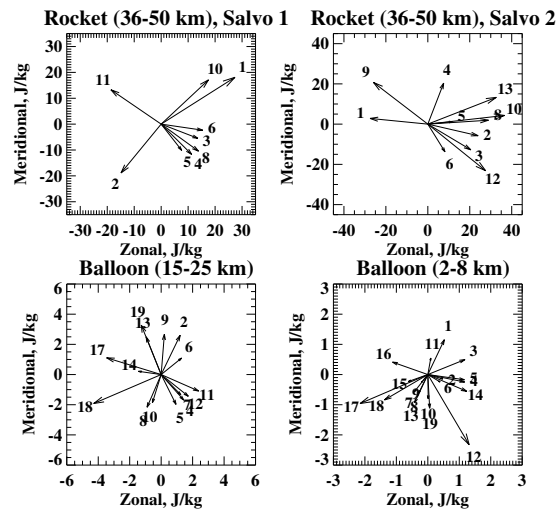


Figure 3. Gravity wave directionality analysis results for the rocket and balloon soundings. The directions of the arrows represent the directions of the horizontal phase propagation of each of the soundings, while the lengths of the arrows correspond to the kinetic energy densities (J kg^{-1}) averaged over the given altitude range (see text for details).

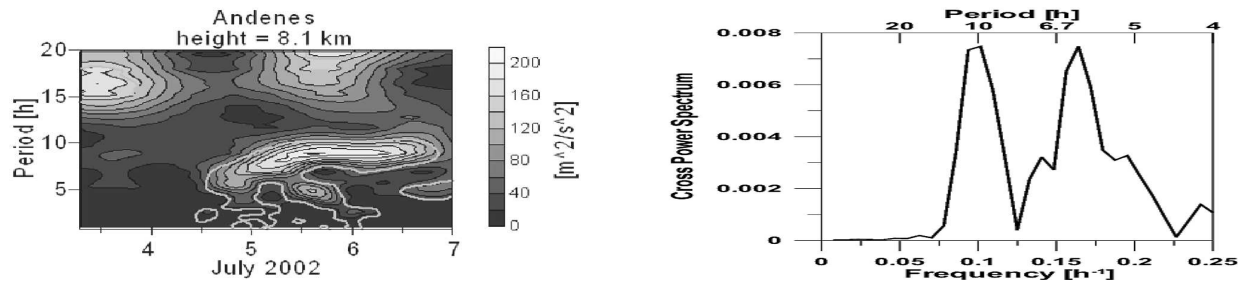


Figure 4. Left panel: Time series of the spectrum of observed period at 8.1 km altitude calculated from the radar data. Right panel: Cross-correlation for the radar wind measurements at Andenes and Kiruna. Two waves with an observed period of ~ 6 hr and ~ 11 hr were seen above both sites (see text).